Meteotsunamis in Orography-Free, Flat Bathymetry and Warming Climate Conditions

Cléa Denamiel[1*], Iva Tojčić[2] and Ivica Vilibić[2]

[1]Ruđer Bošković Institute, Division for Marine and Environmental Research, Bijenička cesta 54, 10000 Zagreb, Croatia
[2]Institute of Oceanography and Fisheries, Šetalište I. Meštrovića 63, 21000 Split, Croatia

[*]Corresponding author: Cléa Denamiel (cdenami@irb.hr)
ORCiD: 0000-0002-5099-1143

Key Points

- Orography of the Apennine mountains does not strongly impact the meteotsunami genesis in the Adriatic Sea
- Flattening of the deepest part of the Adriatic Sea diverts the meteotsunami waves from the sensitive harbour locations
- Extreme climate warming could increase the meteotsunami wave intensities along the most sensitive Adriatic coastal areas

Abstract

Due to a lack of appropriate modelling tools, the atmospheric source mechanisms triggering the potentially destructive meteotsunami waves – occurring at periods from a few minutes to a few hours – have remained partially unstudied till recently. In this numerical work we thus investigate and quantify the impacts of orography and extreme climate changes on the generation and propagation of the atmospheric pressure disturbances occurring during six different historical meteotsunami events in the Adriatic Sea. Additionally, the impact of the bathymetry, and hence the Proudman resonance, on the propagation of the meteotsunami waves is also assessed for the same ensemble of events. Our main findings can be summarized as follow: (1) removing the mountains does not strongly affect the generation nor the propagation of the meteotsunamigenic disturbances but can slightly increase their intensity particularly over the land, (2) climate warming under extreme scenario has the potential to increase the intensity of both atmospheric disturbances and meteotsunami waves in the vicinity of the sensitive coastal areas while (3) flattening the bathymetry of the deepest Adriatic Sea tends to divert the meteotsunami waves from the sensitive harbour locations. Such sensitivity studies, if generalized to other geographical locations with a higher number of events, may provide new insights concerning the still unknown physics of the meteotsunami genesis and, consequently, help to better mitigate meteotsunami hazards worldwide.

Keywords

Meteotsunamigenic disturbances; Apennine mountains; Extreme climate warming; Proudman resonance; Adriatic Sea

Plain Language Summary

Among extreme sea-level hazards, meteotsunami waves – occurring at periods from a few minutes to a few hours – remain the least investigated due to a lack of appropriate high-resolution modelling tools. Consequently, neither the impact of orography and bathymetry on meteotsunamigenic disturbances and meteotsunami waves nor their properties in a projected future climate have been properly quantified. In this numerical work we analyse these impacts, through sensitivity experiments for six different meteotsunami events in the Adriatic Sea. We found that meteotsunamigenic disturbances are not strongly modulated by the orography which can reinforced their intensity, but could be largely increased with extreme climate warming. Further, flattening the bathymetry of the deepest ocean parts tends to divert the meteotsunami waves from the sensitive harbour locations. As meteotsunami events have the potential to cause substantial human and structural damages, this type of studies may be critical to assess and mitigate coastal hazards worldwide.

1 Introduction

In the past decades, the theoretical research on potentially destructive meteorological tsunami events or meteotsunamis – atmospherically-driven long-waves in the tsunami frequency band – has been principally focusing on the atmospheric and resonant processes responsible for the wave generation, the transfers of energy between atmosphere and ocean, as well as the impact of the bathymetry on the ocean wave propagation and amplification (Vilibić et al., 2016). At present, a solid knowledge has been built concerning the atmospheric synoptic conditions favourable to meteotsunami events (Ramis and Jansà, 1983; Vilibić and Šepić, 2017), the different type of ocean resonances (Proudman, 1929; Hibiya and Kajiura, 1982), the energy transfers (Monserrat et al., 1998; Denamiel et al., 2018), the different type of atmospheric disturbances and their propagation (Belušić et al., 2007; Tanaka, 2009; Horvath and Vilibić, 2014) and the bathymetric effects (Rabinovich, 2009; Williams et al., 2020).

But, despite the growing scientific and computational advances, the source mechanisms and generation of the atmospheric pressure disturbances triggering the meteotsunami waves are still not fully understood. One of the major limitations faced by the meteotsunami community is that both observational networks and numerical models are generally not appropriately designed to capture the highly spatially and temporarily varying atmospheric mesoscale structures generating the meteotsunamigenic disturbances (Vilibić et al., 2016; Plougonven and Zhang, 2014; Rabinovich et al., 2020). Nevertheless, the recent implementation of meteotsunami early warning system prototypes (Renault et al., 2011; Denamiel et al., 2019a, 2019b; Anderson and Mann, 2020; Mourre et al., 2020) has demonstrated that kilometre-scale atmospheric models can reproduce some pressure disturbances during meteotsunami events, even though not necessarily at the right geographical locations. Consequently, notwithstanding their potential incapacity to trigger the adequate response of the ocean models at sensitive locations where the events were reported, these atmospheric models can be useful tools to better understand the factors influencing the meteotsunami genesis.

In the meteotsunami community, the Adriatic basin is historically one of the most studied area in the world due to the 21st of June 1978 event when large meteotsunami waves (6 m height for periods of about 20 min) occurred in the Vela Luka harbour and produced substantial damages to the infrastructures (Fig. 1; Vučetić et al., 2009; Orlić et al., 2010). For this region, most of the meteotsunamigenic disturbances are known to develop under similar synoptic conditions (Vilibić and Šepić, 2009; Tojčić et al., 2021) as well as to propagate from the Apennines to the Croatian coasts (Fig. 1) with associated meteotsunami waves travelling across the Adriatic Sea (Vilibić and Šepić, 2009; Denamiel et al., 2020a). However, questions are still raised about (1) the influence of the orography on the generation and propagation of the atmospheric disturbances and (2) their strength in the projected warming climate, (3) the impact of the offshore bathymetry on the propagation of the meteotsunami waves and (4) the relative importance of the travelling meteotsunami waves generated along the Italian coats versus the locally generated waves near the Croatian coasts. Additionally, these questions are also relevant for other meteotsunami hot-spots where they could provide critical input needed to assess both meteotsunami climate and coastal hazards.

To investigate these impacts, we test the meteotsunami genesis and propagation sensitivity by carrying out numerical experiments in the Adriatic Sea (as described in Figure 1) for historical meteotsunami events previously studied with the Adriatic Sea and Coast (AdriSC) atmosphere-ocean operational model (Denamiel et al., 2019a, 2019b). These experiments consist in (1) evaluating the capacity of the AdriSC model to reproduce in re-analysis mode the historical events, (2) testing the impact of the orography on the meteotsunami genesis by removing the Apennines mountains, (3) assessing the impact of far future extreme climate changes on the meteotsunami generation and propagation and (4) analysing the impact of the bathymetry and hence the Proudman resonance by flattening the deepest parts of the Adriatic Sea.

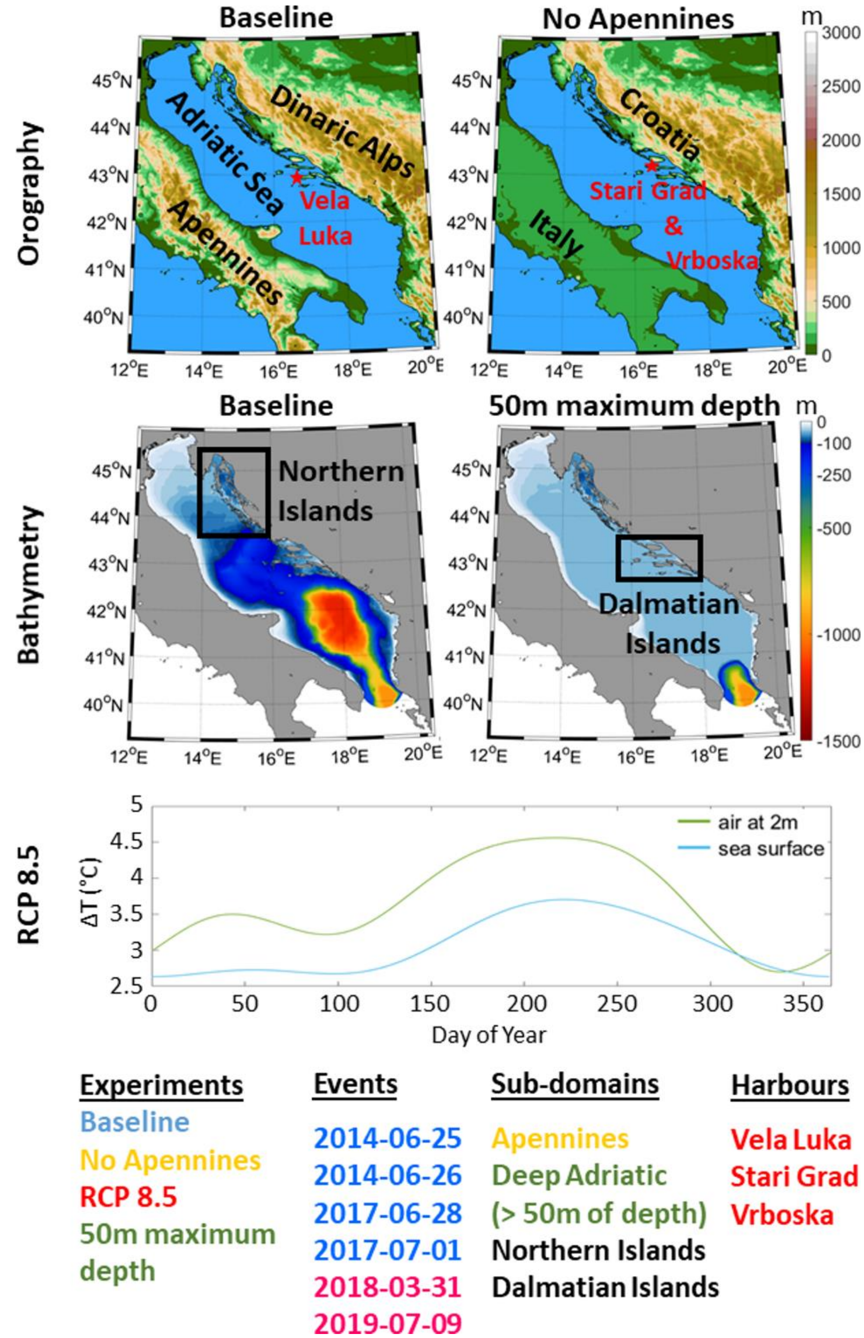

Figure 1. Experimental design of the study. Orography of the atmospheric models (top panels), bathymetry of the ocean models (middle panels) and daily climatology of the temperature changes (ΔT) under climate scenario RCP 8.5 over the atmospheric and ocean domains (bottom panel) used for the four experiments (*Baseline*, *No Apennines*, *RCP 8.5* and *50m maximum depth*), the six studied meteotsunami events (i.e. four *Calm Weather* events: 25th and 26th of June 2014, 27th of June 2017, 1st of July 2017 and two *Stormy Weather* events: 31st of March 2018 and 9th of July 2019), the four chosen sub-domains (*Apennines*, *Deep Adriatic*, *Northern Islands* and *Dalmatian Islands*) and the three sensitive harbour locations (Vela Luka, Stari Grad and Vrboska).

Hereafter, we present in detail the methods used in this study (Section 2) and we investigate both the atmospheric pressure disturbances and the resulting meteotsunami waves, obtained for the numerical simulations of the chosen events, by performing three different kind of analyses (Section 3). First, the regional impacts are spatially presented over the entire Adriatic domain, to see eventual patterns in strengthening or weakening of the meteotsunamigenic disturbances and resulting meteotsunami waves. Then, the distributions of the extremes for each experiment are statistically investigated for the entire set of meteotsunami events, depending on four different sub-domains important for the meteotsunami genesis, propagation and inundation. These statistics also take into account two types of weather conditions found during meteotsunami events (Rabinovich, 2020). Finally, as meteotsunami waves are extremely sensitive to the local nearshore geomorphology, a spectral analysis is carried out at known sensitive harbour locations for specific events well captured by the AdriSC modelling suite.

2 Methods

2.1 AdriSC modelling suite

The Adriatic Sea and Coast (AdriSC) modelling suite has been recently implemented to accurately simulate the atmospheric and oceanic processes driving the Adriatic basin circulation at scales varying from the long-term regional climate changes to the minute-by-minute impact of extreme events along the coasts (Denamiel et al., 2019a). Due to the modular approach developed within the system, the AdriSC modelling suite can operate in both operational and research modes and has already been successfully used in various applications such as climate warming research (Denamiel et al., 2020b, 2020c, 2021) or operational forecast within the Croatian Meteotsunami Early Warning System (CMeEWS; Denamiel et al., 2019a, 2019b; Tojčić et al., 2021).

In this study, we use the AdriSC meteotsunami component with both basic and nearshore modules as described in Denamiel et al. (2019a). The kilometre-scale regional circulation over the Adriatic-Ionian basin is thus derived with the Coupled Ocean-Atmosphere-Wave-Sediment Transport (COAWST) modelling system (Warner et al., 2010) with hourly results at resolutions up to 3-km for the Weather Research and Forecasting (WRF) model (Skamarock et al., 2005) in the atmosphere and 1-km for the Region Ocean Modeling System (ROMS; Shchepetkin and McWilliams, 2005, 2009) in the ocean. However, the 1-min meteotsunami results presented in this article are derived over the entire Adriatic basin with the WRF model at 1.5-km resolution for the atmosphere (domain presented for the orography in Figure 1) and the 2DDI ADvanced CIRCulation (ADCIRC) model (Luettich et al., 1991) using a mesh of up to 10-m resolution in the areas sensitive to meteotsunami hazard for the ocean (domain presented for the bathymetry in Figure 1). Both WRF 1.5-km and ADCIRC models are initialized and forced with the WRF 3-km and ROMS 1-km hourly COAWST results thus minimizing the impact of large-scale boundary effects within the Adriatic basin.

2.2 Experimental design

In this research, the following numerical experiments have been conducted with the AdriSC modelling suite: *Baseline*, *No Apennines*, *RCP 8.5* and *50m maximum depth*. The *Baseline* experiment is carried out in re-analysis mode with (1) realistic orography and bathymetry (Fig. 1) and (2) the COAWST model forced and initialized with the 6-hourly ERA-Interim reanalysis fields (Dee et al., 2011) in the atmosphere and the daily re-analysis MEDSEA-Ocean fields (Pinardi et al., 2003) in the ocean. The *No Apennines* experiment is designed to test the impact of the mountains on the meteotsunami genesis. It is similar to the *Baseline* experiment but the orography of the WRF models is modified in order to flatten the Apennine mountains to 150 m of height (Fig. 1). The *RCP 8.5* experiment follows the pseudo-global warming methodology presented in Denamiel et al. (2020a) which add, to the initial and boundary conditions used in the *Baseline* experiment, the climatological changes due to the expected warming in the Representative Concentration Pathway (RCP) 8.5 scenario for the 2070-2100 period (e.g. the temperature climatological changes – ΔT – are presented for both atmosphere and ocean in Figure 1). Finally, the *50m maximum depth* experiment is carried out as the *Baseline* experiment but with the bathymetry of the ROMS and ADCIRC models modified in order to flatten the deepest part of the Adriatic Sea to 50 m of depth (Fig. 1) to test the impact of the Proudman resonance (Proudman, 1929; Hibiya and Kajiura, 1982) at about 22 m/s (i.e. $C = \sqrt{gH} \approx 22$ m/s with the depth $H = 50$ m and the gravitational acceleration $g \approx 9.81$ m/s^2) on the meteotsunami wave intensity and propagation.

Despite being regular events in the Adriatic Sea, only few well-documented historical meteotsunami events were numerically reproduced with realistic forcing due to the lack of appropriate observational networks and numerical models. In this work we chose to study six events previously simulated with the AdriSC modelling suite used in operational mode (Denamiel et al., 2019a, 2019b), occurring on the 25th and 26th of June 2014, the 28th of June 2017, the 1st of July 2017, the 31st of March 2018 and finally, the 9th of July 2019. It should be noticed that this ensemble of events may be too small to extract entirely robust statistics but can be used to quantify the impact of the chosen orography, bathymetry and climate changes on these specific meteotsunamis and draw some preliminary conclusions.

For each year and each experiment, the COAWST simulation starts 2 days before the first meteotsunami event of the studied year and continuously runs to cover all historical meteotsunami events, while the WRF 1.5-km and ADCIRC simulations start 36 hours later and run till the end of the COAWST simulation. Specifically, the COAWST simulations start at 00:00:00 UTC (1) on the 23th of June for a duration of 4 days in 2014, (2) on the 26th of June for a duration of 6 days in 2017, (3) on the 29th of March for a duration of 3 days in 2018 and finally, (4) on the 7th of July for a duration of 3 days in 2019. All experiments and events including, a total of 24 days of results are thus analysed hereafter.

2.3 Data analysis

In this study we analyse the 1-min results of both the mean sea-level pressure in the atmosphere and the sea-level height in the ocean over a period of 24 hours (starting at 22:00:00 UTC the day before the event) for a total of 24 events (six meteotsunami events for four experiments).

First, the 1-min results are post-processed by applying a Lanczos high-pass filter (Lanczos, 1956) with a 2-h cut-off period. The Lanczos filter is a Fourier method of filtering digital data designed to reduce the amplitude of the Gibbs oscillation. The resulting filtered air-pressure and filtered sea-level height spatial fields are presented in supplementary material (videos S1 to S6). The air-pressure rate of change (or pressure jump) is defined as the time derivative of the filtered mean sea-level pressure over a 4 min period (Denamiel et al., 2019b). Throughout this work, the atmospheric disturbances are defined with the 1-min air-pressure rate of changes (i.e. pressure jumps) and the meteotsunami waves with the 1-min filtered sea-level heights.

Second, the regional changes coming from the experiments are presented for the maximum over time of the air-pressure rate of change and the filtered sea-level height results for each event, as (1) their spatial variations coming from the *Baseline* experiment and (2) the relative changes (in percentage) defined by the biases between the *No Apennines*, *RCP 8.5* or *50m maximum depth* experiments and the *Baseline* experiment normalized by the *Baseline* experiment.

Then, in order to perform some statistical analyses, the Adriatic basin is divided in four sub-domains: (1) *Apennines* which covers the area where the Apennine mountains are flatten to 150 m in the *No Apennines* experiment, (2) *Dalmatian Islands* as well as (3) *Northern Islands* which are only defined over the sea within the areas presented in Figure 1 and, finally, (4) *Deep Adriatic* which covers the sea area where the bathymetry of the Adriatic Sea is flatten to 50 m depth but excludes the parts of the domain already covered by the *Dalmatian Islands* and *Northern Islands* sub-domains. Additionally, two types of meteotsunami events are distinguished following the classification by Rabinovich (2020) based on the type of atmospheric processes triggering the meteotsunami waves. The *Calm Weather* conditions mostly refer to wave-ducting mechanism maintained in the middle troposphere (Lindzen and Tung 1976; Monserrat and Thorpe, 1996) while the *Stormy Weather* conditions occur throughout the whole troposphere with a burst at the surface (e.g. wave-CISK, Belušić et al., 2007; squall lines, Churchill et al., 1995; frontal zones, Proudman, 1929; hurricanes, Shi et al., 2020). Hereafter, the 25th and 26th of June 2014, 28th of June 2017 and 1st of July 2017 are referred as *Calm Weather* events, with calm weather at the ground level and extremely energetic wind conditions at 500 hPa of height, while the 31st of March 2018 and the 9th of July 2019 are referred as *Stormy Weather* events with wind storms at the ground. Within the four selected sub-domains and for the four experiments, statistics for both air-pressure rate of change in the atmosphere and filtered sea-level height in the ocean are presented as (1) violin plots (Hintze and Nelson, 1998) of the distributions of the 98th percentile calculated for the entire duration of the events at each point of the sub-domain, depending on the two event sub-categories and (2) time variations of the 98th percentile calculated every minute for all points of the sub-domain, depending on the six studied events.

Finally, as the amplification of the meteotsunami waves highly depends on the local geomorphology of the sensitive locations, a spectral analysis is performed for the 1-min filtered mean sea-level height results in Stari Grad for the 25th of June 2014 event, in Vela Luka for the 28th of June 2017 and in Vrboska for the 9th of July 2019. For this analysis, the wavelet power spectra in the time-period domain are used to illustrate the temporal change of the variance contained at different periods for the *Baseline* experiment. Similarly, the wavelet coherences in the period-time domain are used to show how the *No Apennines*, *RCP 8.5* and *50m maximum depth* experiments are correlated to the *Baseline* experiment. The presented results for these spectra are nearly all in the period-time domain at which the variability of the signal is significant (i.e. within the 95% confidence level against red noise represented with black lines). We used the Matlab toolbox by Grinsted et al. (2010) to compute and plot normalized Morlet wavelet power spectra and wavelet coherences for the continuous wavelet transform.

Additionally, it is important to notice that, as the atmospheric *Baseline* experiment fields are not changed for the *50m maximum depth* experiment, only the results of the filtered sea-level height are presented in this work for the latter. Similarly, as the *Apennines* sub-domain is entirely located over the land, only the air-pressure jump results are presented for this sub-domain.

3 Results

3.1 Modelled meteotsunami events

The six historical meteotsunami events selected in this study took place in the middle Adriatic basin and were responsible for major flooding in at least one of the three selected sensitive harbour locations of Vela Luka, Stari Grad and Vrboska (Fig. 1) – except for the 26th of June 2014 event which flooded the southern Croatian cities of Rijeka dubrovačka and Ston. For example, eyewitnesses and/or tide gauge measurements reported maximum elevations reaching up to 1.5 m the 25th of June 2014 in Vela Luka, 0.75 m the 28th of June 2017 in Stari Grad and 0.75 m the 25th of June 2014 in Vrboska (Šepić et al., 2016).

These well-documented events have also been previously used to assess the performance of both the meteotsunami forecast component of the Adriatic Sea and Coast (AdriSC) modelling suite (Denamiel et al., 2019a) and the stochastic surrogate model of the CMeEWS (Denamiel et al., 2019b, 2020a; Tojčić et al., 2021). These evaluations performed against a set of up to 48 air-pressure sensors and 19 tide gauges revealed that, in forecast mode, (1) the WRF 1.5-km model could always reproduce some meteotsunamigenic disturbances but not necessarily their proper intensity or direction of propagation, (2) the ADCIRC model could fail to capture the observed meteotsunami waves when the modelled atmospheric disturbances were even slightly shifted in location and (3) the surrogate model could conservatively assess the meteotsunami hazards despite the shortcomings of the AdriSC deterministic forecasts.

In the presented sensitivity analysis, however, our aim is not to perfectly reproduce these six meteotsunami events but to compare the impact of orography, bathymetry and climate change on the atmospheric disturbances and the resulting meteotsunami waves. In order to visually qualify the capacity of the AdriSC model to simulate these impacts, the 5-min evolution of the filtered mean sea-level pressures (i.e. proxy for the atmospheric disturbances) and associated filtered sea-level height (i.e. proxy for the meteotsunami waves) for the *Baseline*, *No Apennines*, *RCP 8.5* and *50m maximum depth* experiments are presented as supplementary material with one mp4 video per event (videos S1 to S6). These videos reveal that, while the 25th of June 2014, 26th of June 2014 and 9th of July 2019 events are likely to be well reproduced, the modelled atmospheric disturbances of the 28th of June 2017 event are too south to affect the Stari Grad harbour which was actually flooded, and are instead likely to trigger meteotsunami waves in the Vela Luka harbour. Finally, for both the 1st of July 2017 and 31st of March 2018 events, the intensities of the reproduced meteotsunami waves are far too low to properly generate any flooding. However, these events may still be used to quantify the impact of the climate change and the Apennines removal on the atmospheric disturbances and are retained in the analyses.

3.2 Regional analysis

As a first assessment of the sensitivity of the meteotsunami genesis and propagation, the relative changes (in percentage) of the *No Apennines*, *RCP 8.5* and, for the ocean only, *50m maximum depth* experiments are regionally compared to the *Baseline* experiment for each modelled event. Hereafter, the comparison is made for the maxima in time of both air-pressure rates of change (Figs. 2 and 3) and filtered sea-level heights (Figs. 4 and 5).

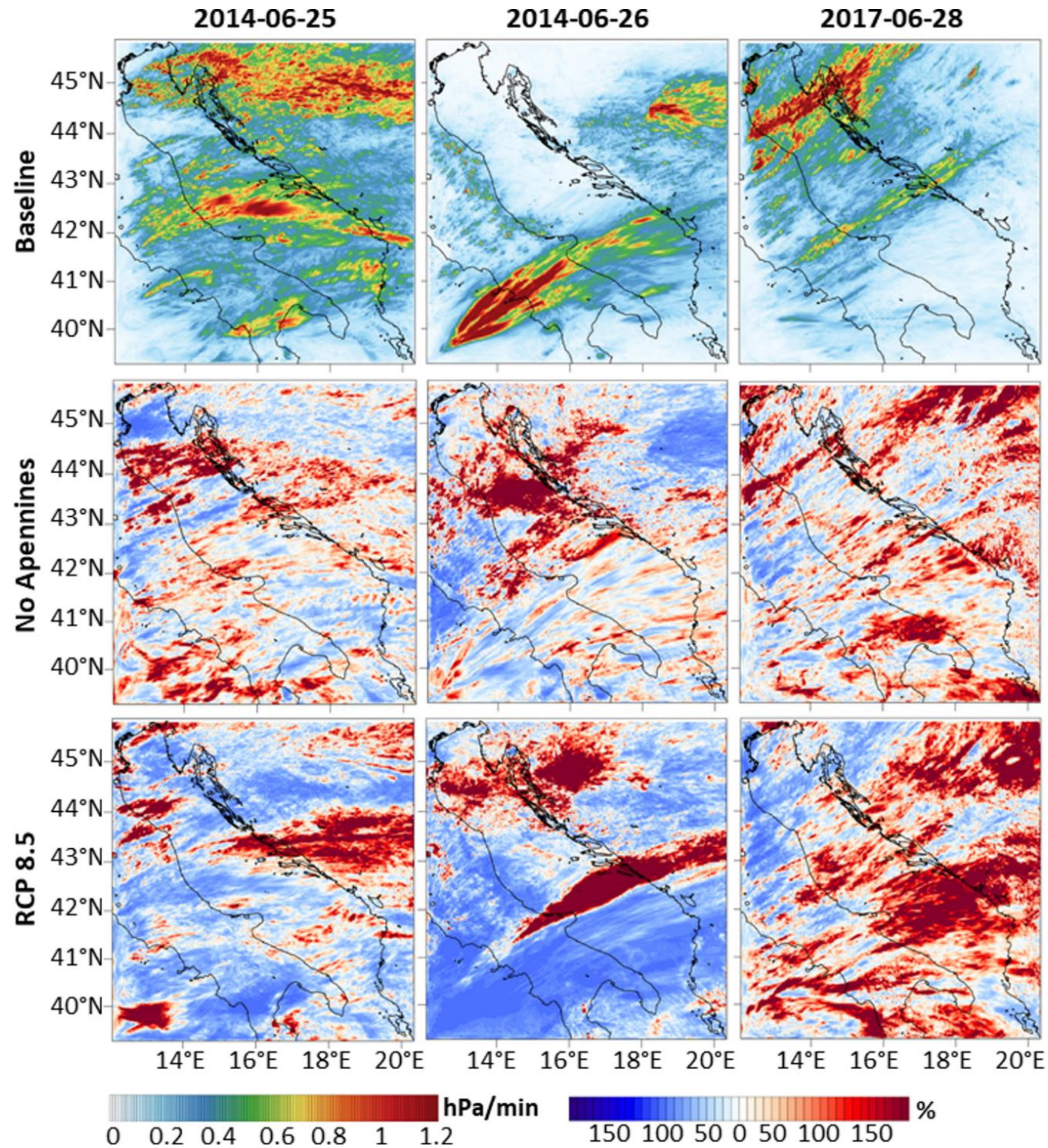

Figure 2. Regional imprint of the sensitivity experiments on the atmospheric pressure disturbances (part 1). *Baseline* maximum air-pressure rates of change (top panels) as well as *No Apennines* (middle panels) and *RCP 8.5* (bottom panels) relative changes (in percentage) for the maximum air-pressure rate of change during the 25th and 26th of June 2014, and 28th of June 2017 events.

For the 25th of June 2014 event, the *Baseline* experiment show the presence of strong atmospheric disturbances (up to 1.2 hPa/min) triggering intense meteotsunami waves (more than 0.10 m) in the middle Adriatic Sea and along the coasts of the *Dalmatian Islands* sub-domain as well as mild atmospheric disturbances in the northern Adriatic Sea. The removal of the Apennine mountains (the *No Apennines* experiment) tends to strongly increase the northern Adriatic atmospheric disturbances (above 150%) and the meteotsunami waves along the coasts of the *Northern Islands* sub-domain (about 100%). It also increases by about 75% the meteotsunamigenic disturbances and about 60% the meteotsunami waves in the middle Adriatic. Under climate warming (the *RCP 8.5* experiment), the baseline atmospheric disturbances decrease by up to 75% and shift northward with an increase by more than 150% of the maximum pressure jumps. Consequently, the maximum filtered sea-level heights are decreased by nearly 100% along the maxima of the *Baseline* meteotsunami waves but increased by more than 100% along the northern coastline of the *Dalmatian Islands* sub-domain. Finally, the impact of the *50m maximum depth* experiment on the meteotsunami waves is mostly to decrease their intensity by up to 70% along the path of the *Baseline* maxima and to divert them towards the southern Adriatic Sea where their intensity is increased by more than 100%.

For the 26th of June 2014 event, strong *Baseline* pressure jumps (more than 1.2 hPa/min) are located in the southern Adriatic Sea and drive travelling meteotsunami waves of about 0.07 m of height, which amplify up to 0.10 m along the south-eastern coasts. As previously, the *No Apennines* experiment is largely increasing the atmospheric disturbances (more than 150%) and the meteotsunami waves (up to 100%) in the northern Adriatic Sea, but mildly changes them (± 70% in the atmosphere and ± 50% in the ocean) along the meteotsunamigenic banners reproduced for the *Baseline* experiment. The changes for the *RCP 8.5* experiment are stronger, with a northward shift of the meteotsunamigenic disturbances revealing an increase of more than 150% and 100% in the air-pressure rates of change and the filtered mean sea-level heights, respectively. Southward, a decrease of these conditions (up to 100% in the atmosphere and 75% in the ocean) occurs. Finally, as previously, the *50m maximum depth* experiment diverts the meteotsunami waves southward (increase of more than 100% of the heights) but also, more surprisingly, northward with up to a 75% increase along the path of the *Baseline* disturbances.

For the 28th of June 2017 event, the *Baseline* atmospheric disturbances occur at two locations: (1) the middle Adriatic with maximum pressure rates of change of about 0.7 hPa/min associated with meteotsunami waves of 0.04 m height and up to 0.1 m along the coasts of the *Dalmatian Islands* sub-domain, as well as (2) the northern Adriatic with maximum pressure jumps above 1.2 hPa/min and meteotsunami waves up to 0.10 m within the *Northern Islands* sub-domain. Both maximum pressure jump and sea-level height increase up to 150% and 100%, respectively, for the *No Apennines* experiment, while, for the *RCP 8.5* experiment, decreasing up to 100% in the northern Adriatic Sea and increasing by more than 100% in the middle and southern Adriatic Sea. As for the 2014 events, the *50m maximum depth* experiment diverts the meteotsunami waves towards the southern Adriatic (more than 100% increase of the maximum height), but also northward from the *Baseline* maximum with a filtered sea-level height increase of about 75%.

For the 1st of July 2017 event, the strongest *Baseline* pressure jumps (up to 1.0 hPa/min) take place northward and southward of the *Dalmatian Islands* sub-domain, in areas where they don't have the potential to generate strong meteotsunami waves in the ocean (maximum filtered sea-level heights below 0.03 m). For the *No Apennines* experiment, the maximum air-pressure rates of change substantially increase (more than 150%) over the Apennine mountains and along the nearshore areas of the *Dalmatian Islands* sub-domain, and decrease by 100% along the southern path of the *Baseline* experiment. Consequently, the meteotsunami waves also increase in the middle Adriatic (more than 100%) but decreased (up to 100%) in the southern Adriatic. The *RCP 8.5* experiment reveals an increase of the atmospheric disturbances (more than 150%) and the meteotsunami waves (more than 100%) in the middle Adriatic and along the *Dalmatian Islands* sub-domain, but a decrease by up to 100% everywhere else. As before, the *50m maximum depth* experiment diverts the meteotsunami waves northward and southward from the path of the Baseline experiment, with up to 100% maximum height increase over these areas.

For the 31st of March 2018 event, the strongest *Baseline* atmospheric disturbances (up to 1.0 hPa/min) are located north of the *Dalmatian Islands* sub-domain and generate moderate meteotsunami waves (up to 0.07 m) mostly along the coasts of the *Northern Islands* sub-domain.

An increase of more than 150% of the pressure jumps as well as between 70% and 100% of the filtered sea-level heights is produced by both *No Apennines* and *RCP 8.5* experiments along the original path of the *Baseline* conditions but also in the nearshore areas of the *Dalmatian Islands* sub-domain. Not surprisingly, the *50m maximum depth* meteotsunami waves are again diverted southward and northward of the path of the *Baseline* waves, with more than 100% maximum height increase over these areas.

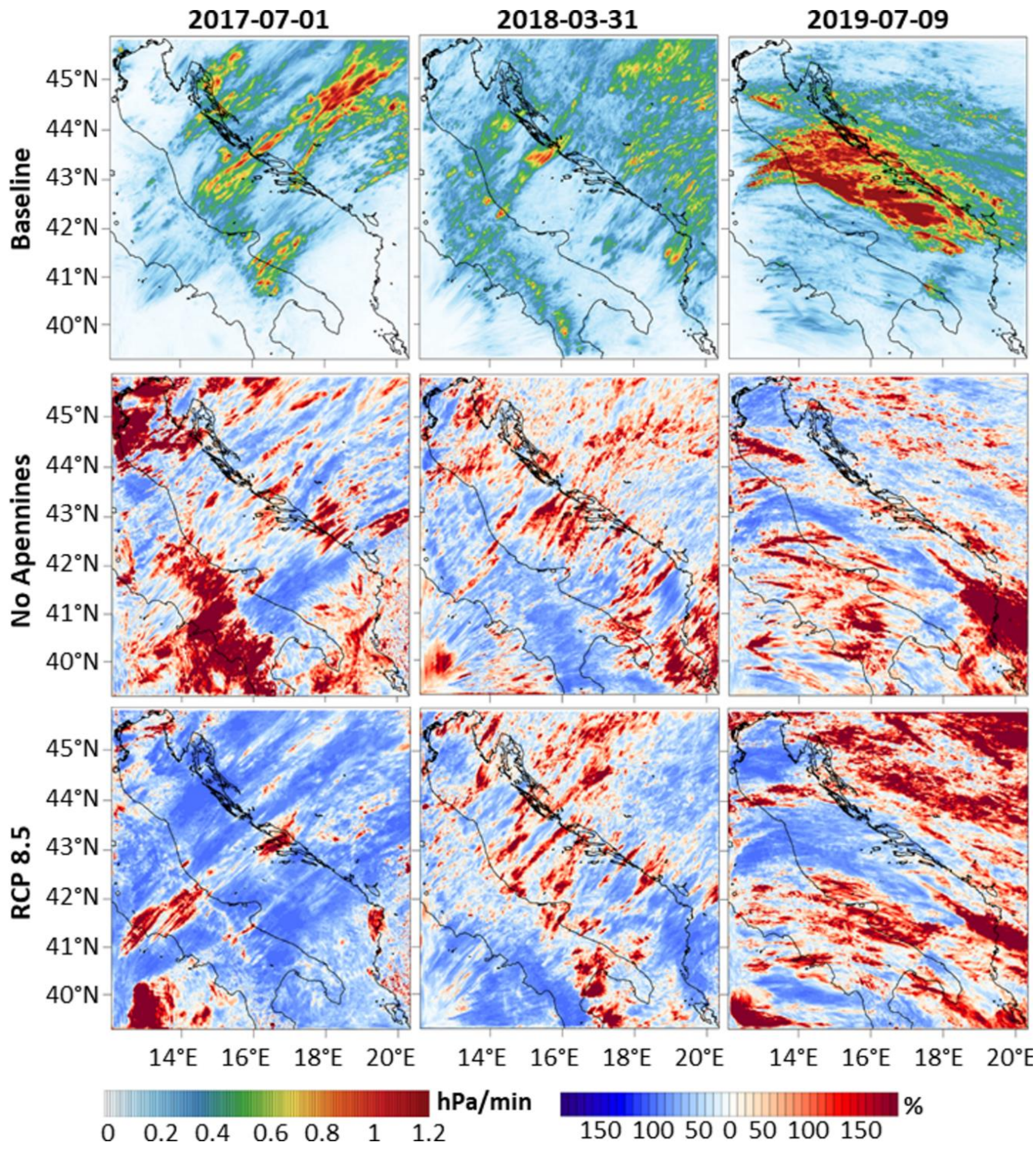

Figure 3. Regional imprint of the sensitivity experiments on the atmospheric pressure disturbances (part 2). Baseline maximum air-pressure rates of change (top panels) as well as No Apennines (middle panels) and RCP 8.5 (bottom panels) relative changes (in percentage) for the maximum air-pressure rate of change during the 1st of July 2017, 31st of March 2018 and 9th of July 2019 events.

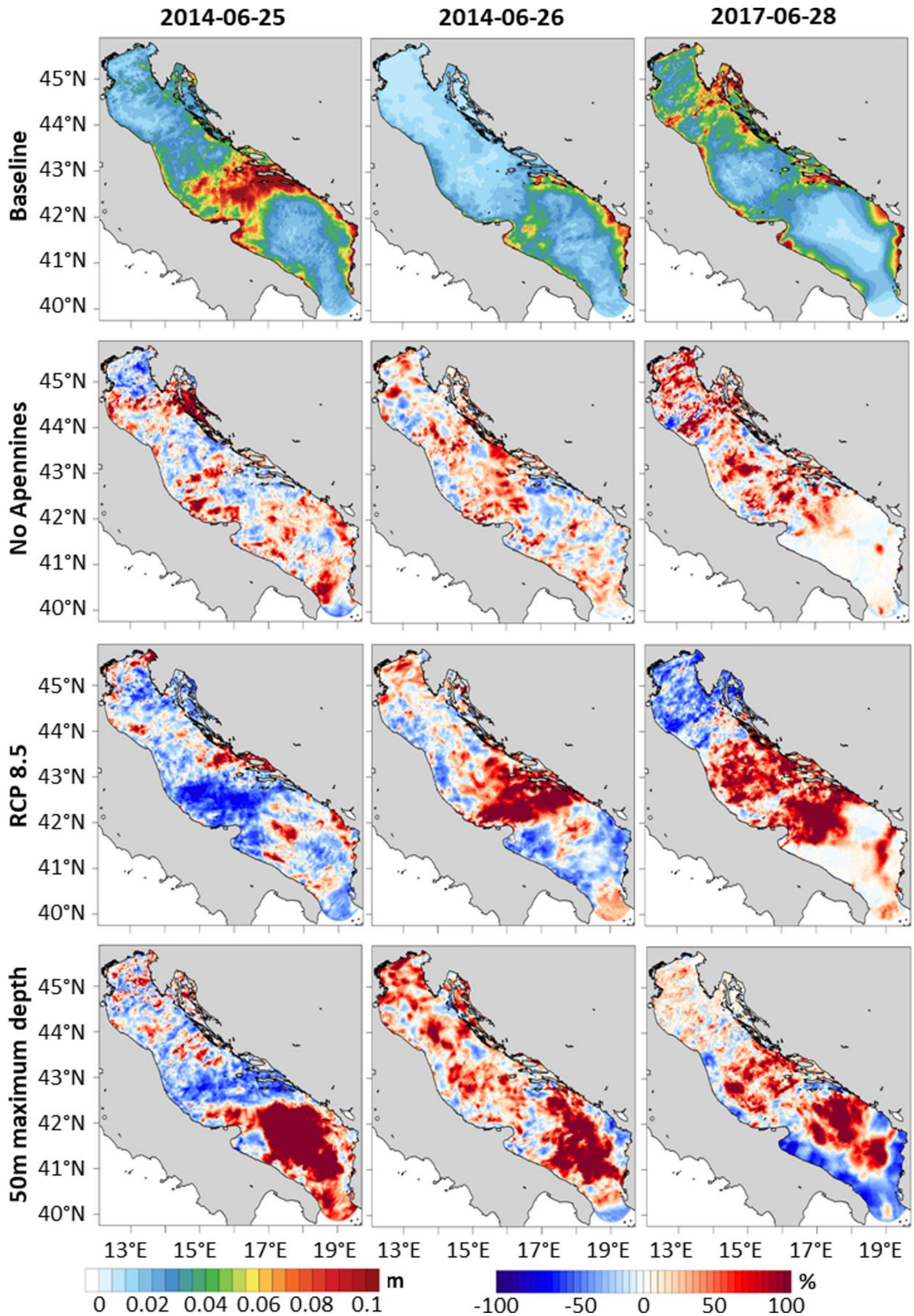

Figure 4. Regional imprint of the sensitivity experiments on the meteotsunami waves (part 1). *Baseline* maximum filtered sea-level height (top panels) as well as *No Apennines* (middle panels), *RCP 8.5* (middle panels) and *50m maximum depth* (bottom panels) relative changes (in percentage) for the maximum filtered sea-level height during the 25th and 26th of June 2014, and 28th of June 2017 events.

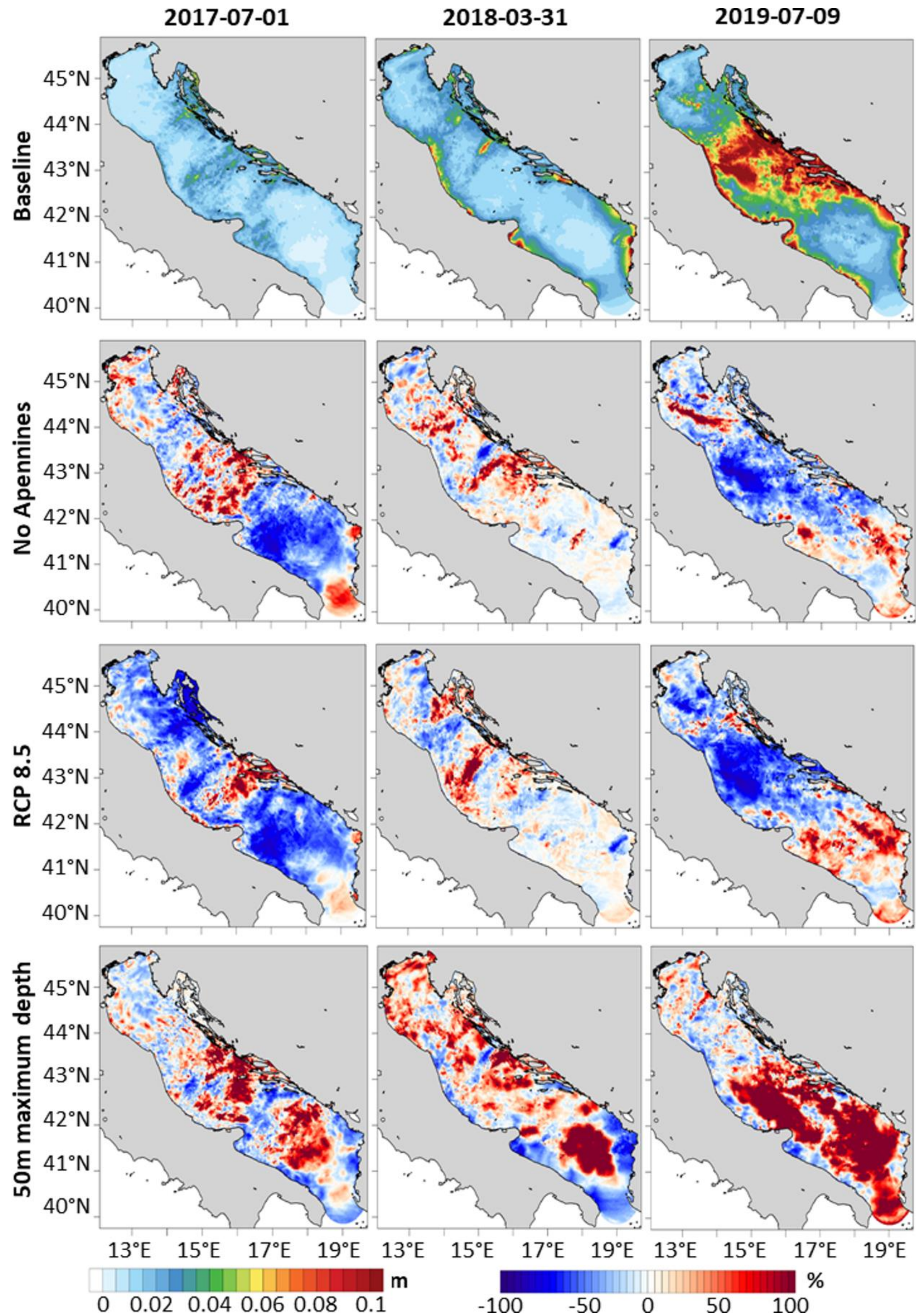

Figure 5. Regional imprint of the sensitivity experiments on the meteotsunami waves (part 2). *Baseline* maximum filtered sea-level height (top panels) as well as *No Apennines* (middle panels), *RCP 8.5* (middle panels) and *50m maximum depth* (bottom panels) relative changes (in percentage) for the maximum filtered sea-level height during the 1st of July 2017, 31st of March 2018 and 9th of July 2019 events.

For the final studied event, the 9th of July 2019, the direction of propagation of the *Baseline* meteotsunamigenic conditions is north-west to south-east, contrarily to the other events that are aligned in direction of meteotsunamigenic banners from south-west to north-east directions. During this storm, the atmospheric disturbances are extremely intense (above 1.2 hPa/min) along the entire coastline of the middle Adriatic basin between 41°N and 44°N of latitude. Consequently, the *Baseline* meteotsunami waves are also extremely strong (above 0.10 m) in this same area. Here, both *No Apennines* and *RCP 8.5* experiments largely decrease the intensity of the *Baseline* experiment (up to 100% in the atmosphere and the ocean) in the open sea and within the nearshore areas of the *Dalmatian Islands* sub-domain for the *RCP 8.5* experiment. However, they both increase the meteotsunami conditions by up to 100% in the southern Adriatic Sea. Additionally, the *50m maximum depth* meteotsunami waves increase more than 100% over the entire Adriatic Sea below 43°N of latitude.

From this regional analysis, we can't draw general conclusions concerning the impacts on meteotsunami conditions of the Apennine mountain removal (the *No Apennines* experiment) or of the extreme climate warming (the *RCP 8.5* experiment) as they seem to vary from event-to-event. Nevertheless, we can conclude that the flattening of the bathymetry (the *50m maximum depth* experiment) always divert the meteotsunami waves from the coasts of the *Dalmatian Islands* sub-domain, where the most destructive meteotsunami events are known to occur.

3.3 Statistical Analysis

In order to better quantify the impact of the different experiments, statistical analyses are performed on four separated sub-domains (*Apennines*, *Deep Adriatic*, *Northern Islands* and *Dalmatian Islands*) for the air-pressure rate of change (i.e. pressure jump) and filtered sea-level height extremes defined as the 98th percentile: (1) in time for all points and two weather type sub-categories (*Calm Weather* and *Stormy Weather*) of events presented as violin plots (Fig. 6), and (2) in space for all times presented as 1-min time series for each event (Fig. 7).

For the *Apennines* sub-domain, the violin plots (Fig. 6) show that over the entire domain for the *Calm Weather* events the pressure jumps increase under the *No Apennines* experiment (i.e. mean value of 0.10 hPa/min instead of 0.09 hPa/min for the *Baseline* experiment and increased number of values above 0.15 hPa/min), but largely decrease for the *RCP 8.5* experiment (i.e. mean value of 0.05 hPa/min and decreased number of values above 0.15 hPa/min). For the *Stormy Weather* events, both *No Apennines* and *RCP 8.5* distributions have a decreased number of values between 0.10 and 0.30 hPa/min compare to the *Baseline* experiment. However, the *RCP 8.5* experiment increase the number of extreme values between 0.30 and 0.80 hPa/min while the *No Apennines* disturbances have no extreme values above 0.30 hPa/min. Similarly, for the time variations of the extremes (Fig. 7), the *RCP 8.5* pressure jumps are mostly weaker than for the *Baseline* and *No Apennines* experiments for the entire duration of the *Calm Weather* events, while the *No Apennines* rate of change peak values (up to 0.35 hPa/min) tend to surpass their *Baseline* counterparts. However, the peaks of the *Stormy Weather* events are higher for the *Baseline* experiment (up to 0.20 hPa/min) than for the *No Apennines* and *RCP 8.5* experiments (below 0.15 hPa/min). This is not necessarily in contradiction with the violin plot distributions showing an increase of extremes over the entire domain for the *RCP 8.5* experiment, as the 98th percentiles over the entire domain and events can be higher than the 98th percentiles for each time of the event.

For the *Deep Adriatic* sub-domain, the violin plot distributions of the air-pressure rates of change are similar to the ones of the *Apennines* sub-domain (Fig. 6). For the *Calm Weather* events, the mean values of the *No Apennines* experiment are similar to the *Baseline* values for the pressure jumps (0.12 hPa/min), while increasing for the filtered sea-level heights (0.019 m vs. 0.017 m for the *Baseline* experiment). For the *RCP 8.5* experiment, the respective mean values are much lower, only 0.09 hPa/min and 0.015 m. However, the respective numbers of extreme values above 0.2 hPa/min and 0.030 m largely increase for the *No Apennines* experiment and decrease in the atmosphere only for the *RCP 8.5* experiment. Additionally, for the *50m maximum depth* experiment, the number of extreme filtered sea-level height values above 0.030 m largely increases compared to the *Baseline* experiment, although the mean values are similar (0.018 m). For the *Stormy Weather* events, both the *No Apennines* and *RCP 8.5* number of extreme pressure jump values decrease above 0.20 hPa/min but increase between 0.10 and 0.20 hPa/min. The respective mean values for all the distributions are about 0.12 hPa/min. In the ocean, mean values for all filtered sea-level height distributions are about 0.019 m while, compared to the *Baseline* experiment, the number of extreme values above 0.030 m are largely increased for the *RCP 8.5* experiment and decreased for both *No Apennines* and *50m maximum depth* experiments. Concerning the time variations (Fig. 7), the *Baseline* pressure jump peaks (up to 0.35 hPa/min) increase (1) for the *No Apennines* experiment (up to 0.50 hPa/min) for the 25th of June 2014, 28th of June 2017 and 31st of March 2018 events and (2) for the *RCP 8.5* experiment (up to 0.40 hPa/min) for the 26th of June 2014 event. In the ocean, the *RCP 8.5* filtered sea-level heights generally increase with respect to the *Baseline* values for the 28th of June 2017, 31st of March 2018 and 9th of July 2019 events. For the 25th and 26th of June events, the *Baseline* filtered sea-level heights decrease under the *RCP 8.5* scenario, but slightly increase under the *No Apennines* and *50m maximum depth* experiments.

For the *Northern Islands* sub-domain, in the atmosphere (Fig. 6), the *No Apennines* pressure jumps clearly increase for the *Calm Weather* events (mean value of 0.14 hPa/min instead of 0.12 hPa/min for the *Baseline* experiment and increased number of values above 0.20 hPa/min, with the maximum reaching 0.80 hPa/min instead of 0.55 hPa/min for the *Baseline* experiment). A strong decrease of the air-pressure rates of change is also seen for the *RCP 8.5* experiment (i.e. mean value of 0.08 hPa/min and decreased number of values between 0.10 and 0.20 hPa/min). Additionally, for the *Stormy Weather* events, the *No Apennines* and *Baseline* distributions are quite similar, while the *RCP 8.5* distribution shows a strong pressure jump decrease (i.e. mean value of 0.14 hPa/min instead of 0.20 hPa/min for the *Baseline* experiment and maximum reaching only 0.55 hPa/min instead of more than 0.8 hPa/min for the *Baseline* experiment). In the ocean, however, all distributions look quite similar for the four experiments. For the time variations (Fig. 7), the *No Apennines* air-pressure rates of change are consistently higher or similar to the *Baseline* values (e.g. reaching the respective values of 1.00 hPa/min and 0.60 hPa/min during the 28th of June 2017). Further, the *RCP 8.5* pressure jumps are always less energetic than the *Baseline* values, except for the 28th of June 2017 when the first peak of the event reaches nearly 0.60 hPa/min instead of 0.30 hPa/min. In the ocean, the peaks of the *No Apennines* and *50m maximum depth* filtered sea-level heights are most of the time higher or similar to the *Baseline* respective values and, for the 28th of June 2017 event, the *RCP 8.5* scenario is characterized by the strongest peak of all *Calm Weather* events, reaching up to 0.135 m.

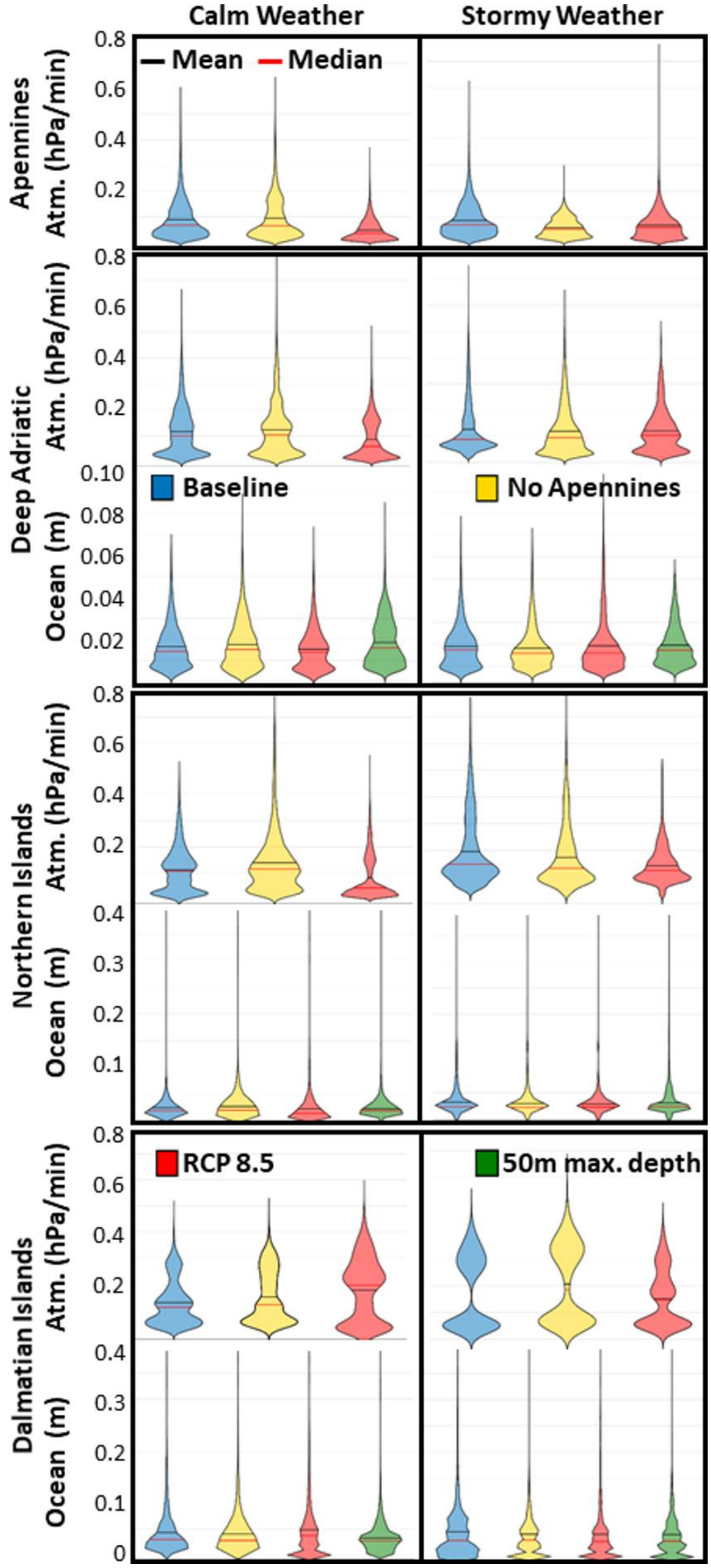

Figure 6. Distributions of the atmospheric disturbance and meteotsunami wave extremes over the four sub-domains. Violin plots of the distributions of the 98th percentile calculated for the entire duration of the events at each point of the four sub-domains (*Apennines*, *Deep Adriatic*, *Northern Islands* and *Dalmatian Islands*) for both the air-pressure rate of change (Atm.) and the filtered sea-level height (ocean). The distributions are presented separately depending on the experiments (*Baseline*, *No Apennines*, *RCP 8.5* and, for the ocean only, *50m maximum depth*) and the weather types (*Calm Weather*, *Stormy Weather*).

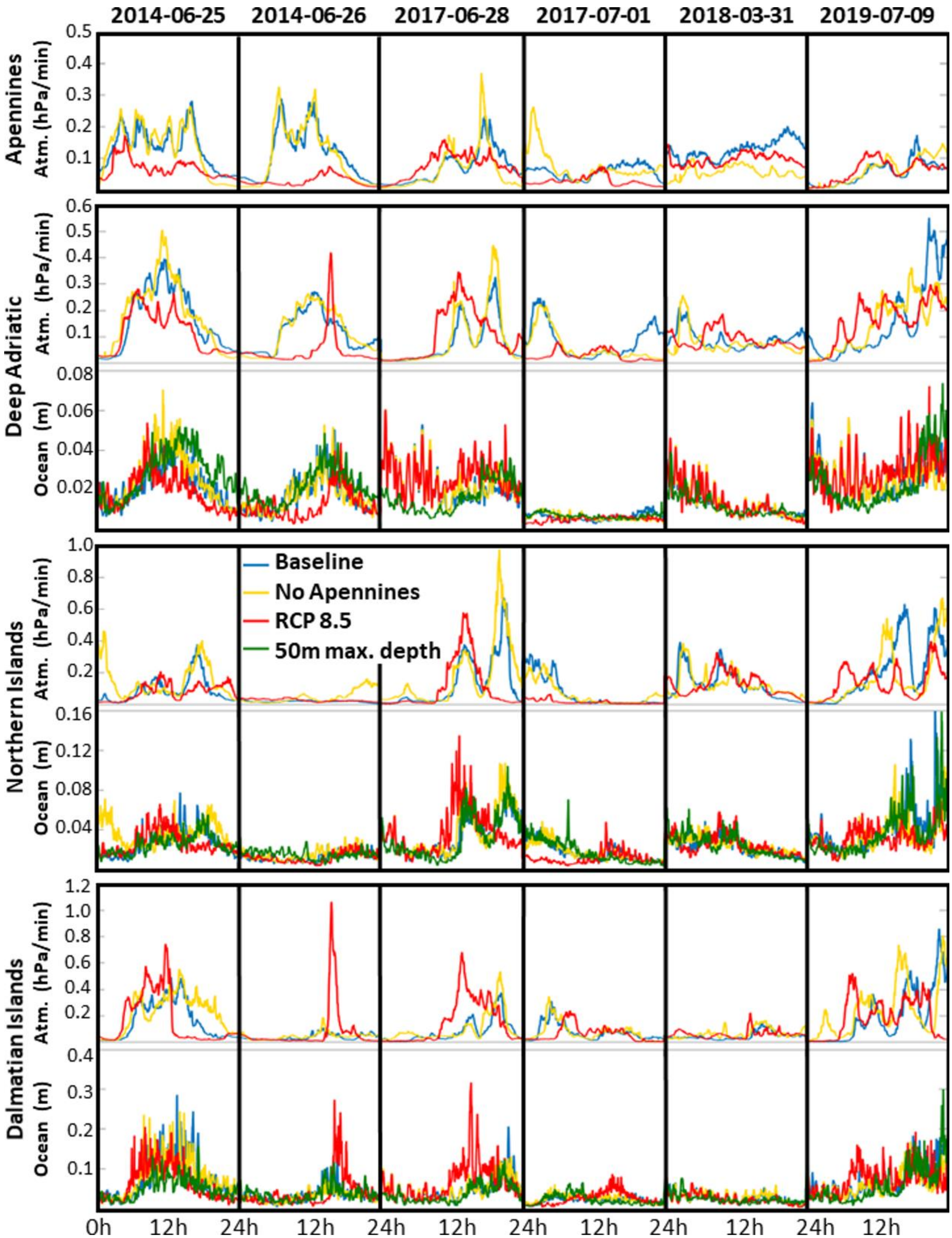

Figure 7. Evolution of the atmospheric disturbance and meteotsunami wave extremes for the four sub-domains. Time variations of the air-pressure rate of change (atm.) and filtered sea-level height (ocean) extreme calculated as the 98th percentile for all points of the four sub-domains (*Apennines*, *Deep Adriatic*, *Northern Islands* and *Dalmatian Islands*) at each time of the events for different experiments (*Baseline*, *No Apennines*, *RCP 8.5* and *50m maximum depth*) and the six studied events.

Finally, within the *Dalmatian Islands* sub-domain, violin plots for the *Calm Weather* events (Fig. 6) show that the air-pressure rates of change increase for the *RCP 8.5* experiment (mean value of 0.17 hPa/min instead of 0.12 hPa/min for the *Baseline* experiment and increased number of values above 0.20 hPa/min). They also increase for the *No Apennines* experiment in both *Calm Weather* (i.e. mean value of 0.15 hPa/min) and *Stormy Weather* (i.e. mean value of 0.21 hPa/min instead of 0.18 hPa/min for the *Baseline* experiment with increased number of values above 0.20 hPa/min) conditions. For the *Stormy Weather* events, the *RCP 8.5* pressure jumps tend to decrease (mean value of 0.15 hPa/min and decreased number of values above 0.20 hPa/min). In the ocean, for the *Stormy Weather* events, the violin plots highlight that the meteotsunami waves largely decrease for the *No Apennines*, *RCP 8.5* and *50m maximum depth* experiments (i.e. mean filtered sea-level heights of 0.042 m for all instead of 0.055 m for the *Baseline* experiment and decreased number of values above 0.050 m). For the *Calm Weather* events, however, only the *RCP 8.5* experiment seems to create stronger meteotsunami waves (i.e. mean filtered sea-level heights of 0.050 m instead of 0.044 m for the *Baseline* experiment and increased number of values above 0.050 m). These changes are well illustrated in the time variation plots (Fig. 7). In the atmosphere, the pressure jump peaks for the *RCP 8.5* experiment largely surpass the ones for the *Baseline* and *No Apennines* experiments for the 25th of June 2014 (0.70 hPa/min instead of 0.55 hPa/min), 26th of June 2014 (1.10 hPa/min instead of less than 0.10 hPa/min) and 28th of June 2017 (0.65 hPa/min instead of respectively 0.40 and 0.50 hPa/min) events. For these events, the atmospheric disturbances generate strong meteotsunami waves with values above 0.150 m: up to 0.250 m for the 25th of June 2014, and up to 0.300 m for the 26th of June 2014 and the 28th of June 2017. For all the events, the *50m maximum depth* filtered sea-level heights tend to largely decrease, with values below 0.100 m for all the events, except during the last hours of the 9th of July 2019 event. Finally, the *No Apennines* filtered sea-level heights also seem to slightly decrease for all the events.

From these statistical analyses, we demonstrate that the atmospheric disturbances increase during the *Calm Weather* events for both *No Apennines* (within the *Apennines* sub-domain) and *RCP 8.5* (within the *Dalmatian Islands* sub-domain) experiments with, consequently, an increase of the meteotsunami waves.

3.4 Spectral Analysis

Because meteotsunami amplification depends on the local geomorphology, the impacts of orography, bathymetry and climate changes to meteotsunami waves is assessed with wavelet and wavelet coherence analyses in the time-period space, for the filtered mean sea-level heights at three sensitive locations (Fig. 1) during three well-reproduced events: in Stari Grad for the 25th of June 2014 event, in Vela Luka for the 28th of June 2017 event and in Vrboska for the 9th of July 2019 event.

Importantly for the meteotsunami propagation, each harbour location has its own amplification factor and resonance frequency. From the time series and the wavelet analyses presented in Fig. 8 for the *Baseline* experiment, it can be seen that Vela Luka has the strongest amplification with meteotsunami waves reaching up to 0.80 m of height for periods of 8 and 17 min for one main peak. The amplifications in Stari Grad and Vrboska are lower reaching up to 0.35 m and 0.50 m of height for periods of 27 min for two main peaks and 12-15 min for three main peaks, respectively. The time series within the harbours confirm the previous results and show that the meteotsunami waves decrease at all locations for the *50m maximum depth* experiment and increased up to nearly 1.00 m in height in Vela Luka for the *RCP 8.5* experiment. The *No Apennines* maximum filtered sea-level heights seem not to change much compared to the *Baseline* values.

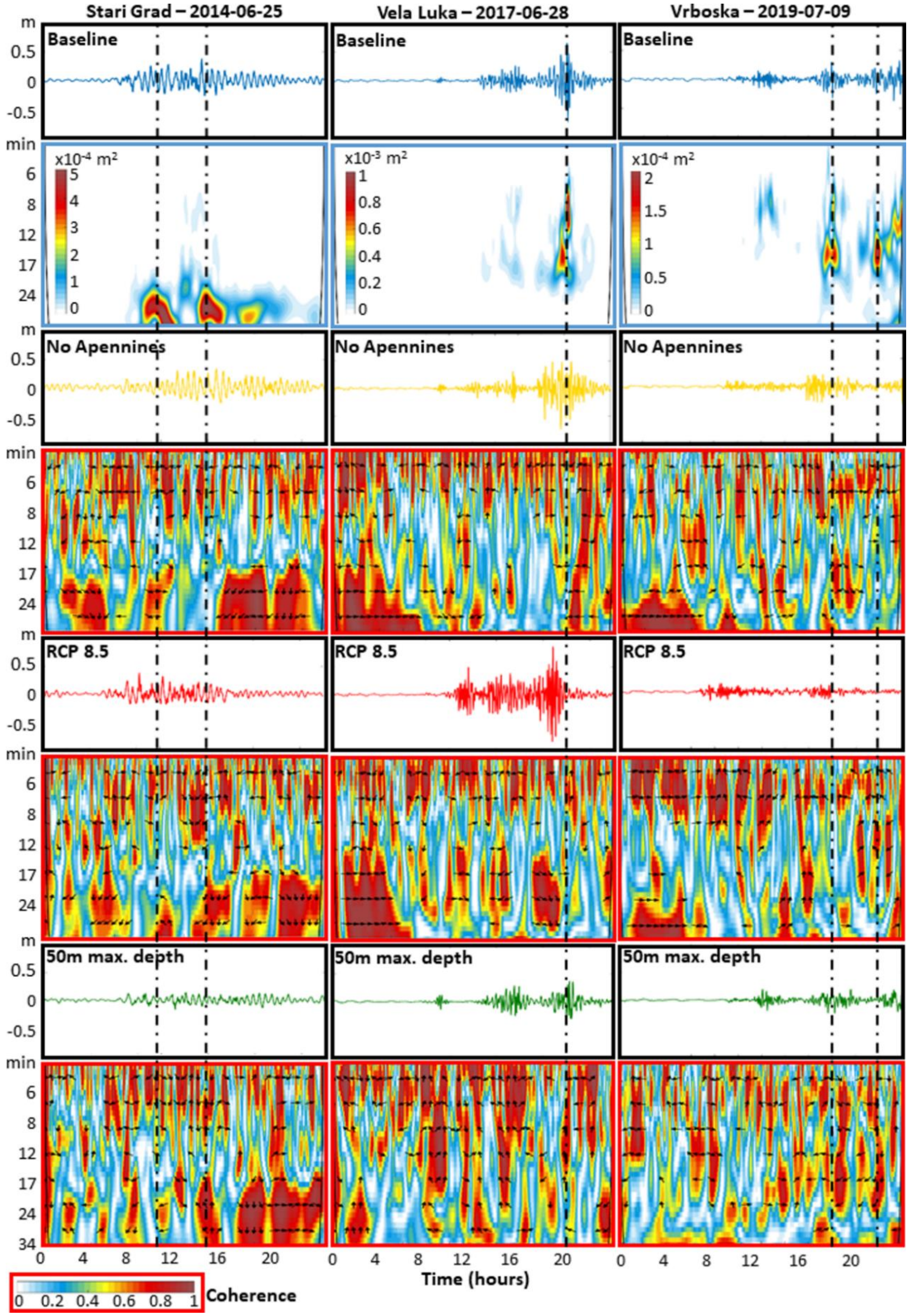

Figure 8. Spectral analysis of the meteotsunami waves in different experiments at sensitive harbour locations. Filtered mean sea-level height time-series (black frames), normalized wavelet power spectrum for the *Baseline* experiment (blue frames) and wavelet coherence for the *No Apennines*, *RCP 8.5* and *50m maximum depth* experiments (red frames) at three sensitive harbour locations along the *Dalmatian Islands* sub-domain for chosen events (Stari Grad for the 25th of June 2014 event, Vela Luka for the 28th of June 2017 event and Vrboska for the 9th of July 2019 event).

Concerning the wavelet coherence analyses in the time-period space, they reveal several interesting features during the meteotsunami events. For the *No Apennines* experiment, the time series of filtered sea-levels often have low interdependences (i.e. coherence below 0.40) to their *Baseline* counterparts and are in anti-phase. In other words, the arrows pointing to the bottom-left show that the *No Apennines* meteotsunami events occur after the *Baseline* events for all the periods between 8 and 27 min, with the exception of the first peaks in Stari Grad and Vrboska. For the *RCP 8.5* experiment, the time series generally have high interdependence (coherence above 0.75) but are not in phase. For the second peak only, meteotsunami events occur after their *Baseline* counterparts in Stari Grad and Vrboska but before in Vela Luka. Finally, for the *50m maximum depth* experiment, the time series always have high interdependence (i.e. coherence above 0.75) but are not in phase, with all events occurring after their *Baseline* counterparts.

The spectral analysis thus reveal that environmental changes are impacting not only the intensity of the events but also their timing and their behaviour in the time-period space.

4 Discussion

In the last century, breakthroughs in computational science and better access to powerful numerical resources have allowed the research community to perform more and more detailed geoscientific studies such as, for example, the impact of climate change on the atmosphere-ocean dynamics (Giorgi, 2019). Recently, in the meteotsunami community, the development of sub-kilometre scale coupled atmosphere-ocean modelling suites capable to reproduce the internal atmospheric gravity waves triggering the meteotsunami events have provided the appropriate tools to quantify the influence of different factors (orography, bathymetry, climate change) on the meteotsunami genesis, thus breaking the barriers of the theoretical, experimental and observational studies. In this work we presented the first results of such a numerical approach.

Our main findings are summarized in Figure 9, presenting the peaks in time (as seen in Figure 7) of both meteotsunami wave and pressure disturbance extremes for each event over each sub-domain (except for the *Apennines* sub-domain which does not cover the Adriatic Sea). They show that:

- meteotsunami-favourable conditions are likely to be largely increased within the *Dalmatian Islands* sub-domain in both atmosphere and ocean under a projected extreme warming climate (*RCP 8.5* experiment). This is particularly relevant as the strongest and most destructive meteotsunami events occur within this sub-domain (Vilibić et al., 2016; Denamiel et al., 2018, 2020a);
- however, meteotsunami waves are projected to decrease in the adjacent *Northern Islands* sub-domain under warmer climate (the *RCP 8.5* experiment). Therefore, meteotsunami-favourable conditions are geographically limited due to, for example, the regional bathymetries (flat bathymetry off the *Northern Islands* sub-domain versus complex and changing bathymetry off the *Dalmatian Islands* sub-domain);
- flattening of the bathymetry (the *50m maximum depth* experiment) substantially decreases the meteotsunami waves in the *Dalmatian Islands* sub-domain, thus indicating that the Proudman resonance (Proudman, 1929) – which is hypothesised to be a major process of the meteotsunami generation (Orlić et al., 2010; Monserrat et al., 2006) – is not playing a substantial role in this region characterized by a changing bathymetry. On the contrary, the flattening is found to divert the meteotsunami waves from the hot-spot locations and to

channelize the meteotsunami energy similarly to tsunami propagation over ridges and channels (Titov et al., 2005);

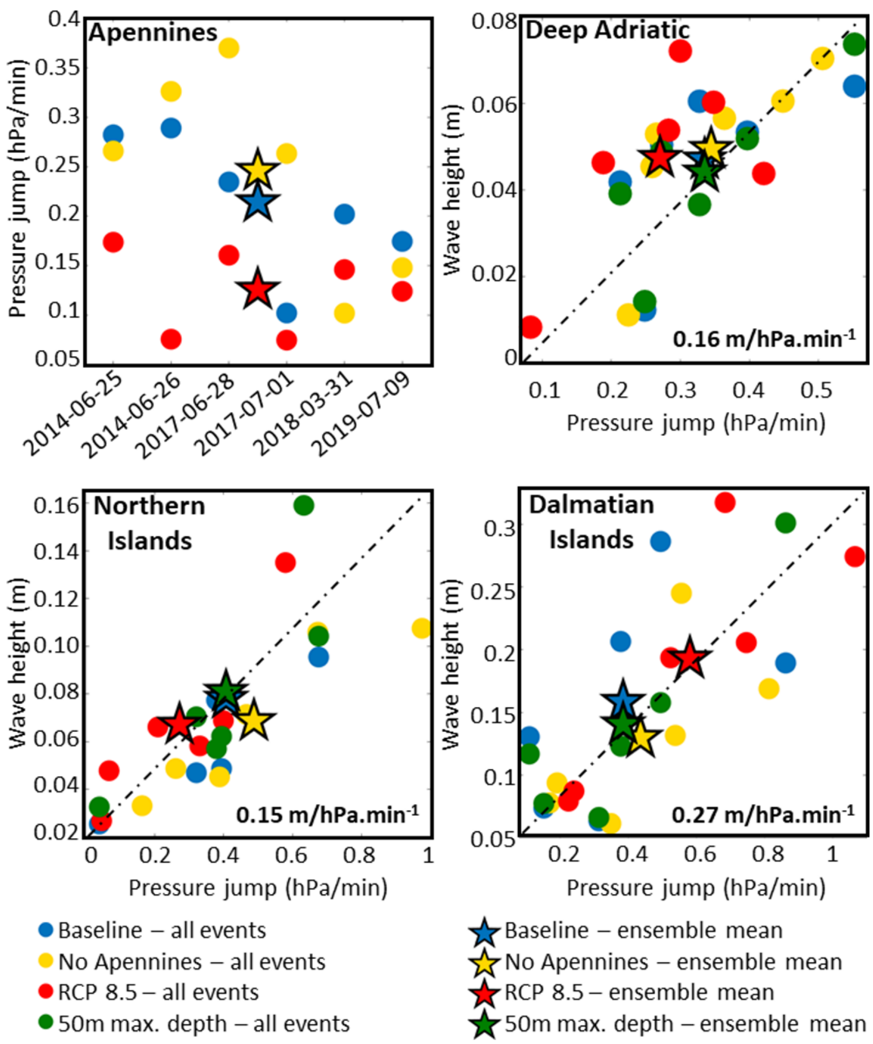

Figure 9. Summary of the findings. For the *Baseline*, *No Apennines* and *RCP 8.5* experiments, peak of the time variations of the 98th percentile for the mean sea-level pressure jump in the atmosphere (as presented in Figure 7) depending on the six selected events for the *Apennines* sub-domain (top left panel). For the four different experiments and all the selected events, peak of the time variations of the 98th percentile for the filtered mean sea-level height (i.e. meteotsunami wave height in the ocean, as presented in Figure 7) depending on the peak of the time variations of the 98th percentile for the air-pressure rate of change in the atmosphere (as presented in Figure 7) for the *Deep Adriatic*, *Northern Islands* and *Dalmatian Islands* sub-domains. For these sub-domains, the linear relationship between the atmospheric disturbance jump and the meteotsunami wave height is given as m/hPa for all events and experiments.

- removing the Apennines (the *No Apennine* experiment) does not substantially change the intensity of the meteotsunamigenic disturbances (except an increase within the *Apennines* sub-domain) but results in different spatial patterns, particularly for the *Calm Weather* situations. In the ocean, the resulting meteotsunami waves are slightly stronger, presumably due to different characteristic of the meteotsunamigenic disturbances (e.g. speed or propagation direction). Therefore, the meteotsunamigenic disturbances are not generated by the orography, just being modulated, while their origin is presumably driven by shear instabilities or similar processes that normally generate atmospheric internal gravity waves (Plougonven and Zhang, 2014). That may apply for other world locations vulnerable to meteotsunami events (e.g. the Balearic Islands) for which mountains are also suspected to have a substantial role in the meteotsunami genesis (Jansá and Ramis, 2020).

The only previous study quantifying the impact of future climate on the meteotsunami generation has been using proxy-derived meteotsunami indices defined at the synoptic scale in the Balearic Islands (Vilibić et al., 2018). Following this work, the number of meteotsunami events is expected to increase by 34% under the RCP 8.5 climate scenario. Yet, contrarily to the approach used in our study, the synoptic meteotsunami index cannot be used to forecast the intensity of these extreme events. Further, in the Adriatic Sea, Vilibić and Šepić (2009) hypothesized that the strong fronts present during meteotsunami events, may be generated or additionally boosted by the orography of the Apennines. However, in our study we demonstrated that the Apennines have little impact on the meteotsunami genesis. Finally, many studies investigated the influence of the bathymetry on the meteotsunami wave generation and propagation around the world, putting the accent to the Proudman resonance as the meteotsunami generation mechanism (Williams et al., 2020; Bubalo et al., 2021). Indeed, the Proudman resonance is the dominant process in regions with flat bathymetries, like wide shelves (Titov and Moore, 2021), but our results indicate that this is not necessarily the case for one of the most vulnerable regions in the world, the coastal middle Adriatic Sea.

Notwithstanding the undeniable interest of this study for the meteotsunami community, our analyses present several critical aspects and our conclusions should not be generalized without caution. First, meteotsunami genesis and propagation highly depend on the studied geographical location and our results may not be valid outside of the Adriatic basin. Then, the ensemble of six events used in this study is not only small but also includes two meteotsunamis that were not properly reproduced with the AdriSC model (Denamiel et al., 2019a). Finally, the found process-level impacts are highly variable from event-to-event depending on the intensity, location and type (i.e. the *Calm Weather* and *Stormy Weather* events) of the meteotsunami conditions. Consequently, we foresee several avenues that can be pursued in future studies to increase the confidence on the presented numerical results. First, the number of events in the studied ensembles should be increased – e.g. the full catalogue of historical meteotsunami events in the Adriatic Sea (Orlić, 2015) should be numerically reproduced. Second, the physics and resolutions of the numerical models should be continuously improved to better capture the coupled atmosphere-ocean meteotsunami dynamics. Then, other geographical locations in the world should be researched – e.g. the Balearic Islands (Jansá and Ramis, 2020), the Korean and Japanese west coasts (Hibiya and Kajiura, 1982; Choi et al., 2014), the U.S. East Coast (Churchill et al., 1995; Wertman et al., 2014). Finally, the atmospheric research should be scaled-up within the meteotsunami community which is mostly composed of oceanographers – e.g. in the Adriatic, only few studies have been led by atmospheric scientists (Belušić et al., 2007; Horvath et al., 2018).

To conclude, we expect that with the constant technological evolutions, sub-kilometre scale coupled atmosphere-ocean models better adjusted to represent meteotsunami events may, in a near future, run at reduced computational cost and allow for radical discoveries concerning the still unknown physics of the meteotsunami genesis.

Acknowledgements and Data

Acknowledgements are made for the support of the European Centre for Middle-range Weather Forecast (ECMWF) staff as well as for ECMWF's computing and archive facilities used in this research. This work has been supported by projects ADIOS and BivACME (Croatian Science Foundation Grants IP-2016-06- 1955 and IP-2019-04-8542, respectively), CHANGE WE CARE (Interreg Italy-Croatia program), and two ECMWF Special Projects (“Using stochastic surrogate methods for advancing towards reliable meteotsunami early warning systems” and “Numerical modelling of the Adriatic-Ionian decadal and inter-annual oscillations: from realistic to process-oriented simulations”). The model results used to produce this article can be obtained under the Open Science Framework (OSF) FAIR data repositories https://osf.io/xmek4/ and https://osf.io/wxm7f/.

References

Anderson, E. J., & Mann, G. E. (2020), A high-amplitude atmospheric inertia–gravity wave-induced meteotsunami in Lake Michigan. *Nat. Hazards*. doi:10.1007/s11069-020-04195-2

Belušić, D., Grisogono, B., & Klaić, Z. B. (2007), Atmospheric origin of the devastating coupled air-sea event in the east Adriatic. *J. Geophys. Res.*, 112, D17111. doi:10.1029/2006JD008204

Bubalo, M., Janeković, I., & Orlić, M. (2021), Meteotsunami-related flooding and drying: numerical modeling of four Adriatic events. *Nat. Hazards*. doi:10.1007/s11069-020-04444-4

Choi, B.-J., Hwang, C., & Lee, S.-H. (2014), Meteotsunami-tide interactions and high-frequency sea level oscillations in the eastern Yellow Sea. *J. Geophys. Res. Oceans*, *119*, 6725– 6742. doi:10.1002/2013JC009788

Churchill, D. D., Houston, S. H., & Bond, N. A. (1995), The Daytona Beach wave of 3–4 July 1992: a shallow water gravity wave forced by a propagating squall line. *Bull. Am. Meteorol. Soc. 76*, 21–32.

Dee, D. P. et al. (2011), The ERA-Interim reanalysis: configuration and performance of the data assimilation system. *Q. J. Roy. Meteorol. Soc.*, *137*, 553–597. doi:10.1002/qj.828

Denamiel, C., Tojčić, I., & Vilibić, I. (2021), Balancing accuracy and efficiency of atmospheric models in the northern Adriatic during severe bora events. *J. Geophys. Res. Atmos.*, *126*, e2020JD033516. doi:10.1029/2020JD033516

Denamiel, C., Tojčić, I., & Vilibić, I. (2020c), Far future climate (2060–2100) of the northern Adriatic air–sea heat transfers associated with extreme bora events. *Clim. Dyn.*, *55*, 3043–3066. doi:10.1007/s00382-020-05435-8

Denamiel, C., Pranić, P., Quentin, F., Mihanović, H., & Vilibić, I. (2020b), Pseudo-global warming projections of extreme wave storms in complex coastal regions: The case of the Adriatic Sea. *Clim. Dyn.*, *55*, 2483–2509. doi:10.1007/s00382-020-05397-x

Denamiel, C., Huan, X., Šepić, J., & Vilibić, I. (2020a), Uncertainty Propagation Using Polynomial Chaos Expansions for Extreme Sea Level Hazard Assessment: The Case of the Eastern Adriatic Meteotsunamis. *J. Phys. Oceanogr.*, *50*(4), 1005-1021. doi:10.1175/JPO-D-19-0147.1

Denamiel, C., Šepić, J., Huan, X., Bolzer, C., & Vilibić, I. (2019b), Stochastic surrogate model for meteotsunami early warning system in the eastern Adriatic Sea. *J. Geophys. Res. Oceans*, *124*, 8485–8499. doi:10.1029/2019JC015574

Denamiel, C., Šepić, J., Ivanković, D., & Vilibić, I. (2019a), The Adriatic Sea and Coast modelling suite: Evaluation of the meteotsunami forecast component. *Ocean Modell.*, *135*, 71–93. doi:10.1016/j.ocemod.2019.02.003

Denamiel, C., Šepić, J., & Vilibić, I. (2018), Impact of geomorphological changes to harbor resonance during meteotsunamis: The Vela Luka Bay test case. *Pure Appl. Geophys.*, *175*(11), 3839–3859. doi:10.1007/s00024-018-1862-5

Giorgi, F. (2019), Thirty years of regional climate modeling: Where are we and where are we going next?. *J. Geophys. Res. Atmos.*, *124*, 5696– 5723. doi:10.1029/2018JD030094

Grinsted, A., Moore, J. C., & Jevrejeva, S. (2010), Application of the cross wavelet transform and wavelet coherence to geophysical time series, *Nonlinear Process. Geophys. 11*, 561–566.

Hibiya, T., & Kajiura, K. (1982), Origin of the Abiki phenomenon (a kind of seiche) in Nagasaki Bay. *J. Oceanogr. Soc. Jpn.*, *38*, 172–182.

Hintze, J. L., & Nelson, R. D., (1998), Violin plots: a box plot-density trace synergism. *Am. Stat.*, *52* (2), 181–184. doi:10.1080/00031305.1998.10480559

Horvath, K., Šepić, J., & Telišman Prtenjak, M. (2018), Atmospheric forcing conducive for the Adriatic: 25 June 2014 meteotsunami event. *Pure Appl. Geophys.*, *175*, 3817–3837. doi:10.1007/s00024-018-1902-1

Horvath, K., & Vilibić, I. (2014), Atmospheric mesoscale conditions during the Boothbay meteotsunami: a numerical sensitivity study using a high-resolution mesoscale model. *Nat. Hazards, 74*, 55–74.

Jansá, A., & Ramis, C. (2020), The Balearic rissaga: from pioneering research to present-day knowledge. *Nat. Hazards*. doi:10.1007/s11069-020-04221-3

Lanczos, C. (1956), Applied Analysis, Prentice Hall, Engle-Wood Cliffs, New Jersey.

Lindzen, R. S., & Tung, K. (1976), Banded convective activity and ducted gravity waves. *Mon. Weather Rev.*, *104*(12), 1602-1617. doi:10.1175/1520-0493(1976)104<1602:BCAADG>2.0.CO;2

Luettich, R. A., Birkhahn, R. H., & Westerink, J. J. (1991), Application of ADCIRC-2DDI to Masonboro Inlet. A brief numerical modeling study. Contractors Report to the US Army Engineer Waterways Experiment Station: North Carolina.

Monserrat, S., Vilibić, I., & Rabinovich, A. B. (2006), Meteotsunamis: atmospherically induced destructive ocean waves in the tsunami frequency band. *Nat. Hazards Earth Syst. Sci.* **6**, 1035–1051. doi:10.5194/nhess-6-1035-2006

Monserrat, S., Rabinovich, A. B., & Casas, B. (1998), On the reconstruction of the transfer function for atmospherically generated seiches. *Geophys. Res. Lett.*, *25*(12), 2197–2200.

Monserrat, S., & Thorpe, A. J. (1996), Use of Ducting Theory in an Observed Case of Gravity Waves. *J. Atm. Sci.*, *53*(12), 1724-1736. doi:10.1175/1520-0469(1996)053<1724:UODTIA>2.0.CO;2

Mourre, B. et al. (2020), On the potential of ensemble forecasting for the prediction of meteotsunamis in the Balearic Islands: sensitivity to atmospheric model parameterizations. *Nat. Hazards*. doi:10.1007/s11069-020-03908-x

Orlić, M. (2015), The first attempt at cataloguing tsunami-like waves of meteorological origin in Croatian coastal waters. *Acta Adriat. 56*, 83–95.

Orlić, M., Belušić, D., Janeković, I., & Pasarić, M. (2010), Fresh evidence relating the great Adriatic surge of 21 June 1978 to mesoscale atmospheric forcing. *J. Geophys. Res. Oceans, 115*, C06011. doi:10.1029/2009JC005777

Pinardi, N. et al. (2003), The Mediterranean ocean forecasting system: first phase of implementation (1998–2001). *Ann. Geophys., 21*, 3–20. doi:10.5194/angeo-21-3-2003

Plougonven, R., & Zhang, F. (2014), Internal gravity waves from atmospheric jets and fronts. Rev. Geophys. 52, 33–76. doi:10.1002/2012RG000419

Proudman, J. (1929), The effects on the sea of changes in atmospheric pressure. *Geophys. Suppl. Mon. Notices R. Astron. Soc., 2*(4), 197–209.

Rabinovich, A. B., Šepić, J. & Thomson, R. E. (2020), The meteorological tsunami of 1 November 2010 in the southern Strait of Georgia: a case study. *Nat. Hazards*. doi:10.1007/s11069-020-04203-5

Rabinovich, A. B. (2020), Twenty-seven years of progress in the science of meteorological tsunamis following the 1992 Daytona Beach event. *Pure Appl. Geophys. 177*, 1193–1230. doi:10.1007/s00024-019-02349-3

Rabinovich, A. B. (2009), Seiches and harbor oscillations. In: Kim, Y.C. (Ed.), Handbook of Coastal and Ocean Engineering. World Scientific Publ, Singapore, pp. 193–236.

Ramis, C., & Jansà, A. (1983), Condiciones meteorológicas simultáneas a la aparición de oscilaciones del nivel del mar de amplitud extraordinaria en el Mediterráneo occidental (in Spanish). *Revista Geofísica, 39*, 35–42.

Renault, L., Vizoso, G., Jansà, A., Wilkin, J., & Tintoré, J. (2011), Toward the predictability of meteotsunamis in the Balearic Sea using regional nested atmosphere and ocean models. *Geophys. Res. Lett., 38*, L10601. doi:10.1029/2011gl047361

Šepić, J., Međugorac, I., Janeković, I., Dunić, N., & Vilibić, I. (2016), Multi-meteotsunami event in the Adriatic Sea generated by atmospheric disturbances of 25–26 June 2014. *Pure Appl. Geophys., 173*, 4117-4138.

Shchepetkin, A. F., & McWilliams, J. C. (2009), Correction and commentary for "Ocean forecasting in terrain-following coordinates: Formulation and skill assessment of the regional ocean modeling system" by Haidvogel et al. J. Comput. Phys. 227, pp. 3595–3624. *J. Comput. Phys., 228*(24), 8985–9000. doi:10.1016/j.jcp.2009.09.002

Shchepetkin, A. F., & McWilliams, J. C. (2005), The regional oceanic modeling system: A split-explicit, free-surface, topography-following- coordinate ocean model. *Ocean Modell., 9*(4), 347–404. doi:10.1016/j.ocemod.2004.08.002

Shi, L., Olabarrieta, M., Nolan, D. S., & Warner, J. C. (2020), Tropical cyclone rainbands can trigger meteotsunamis. *Nat. Commun., 11*, 678. doi:10.1038/s41467-020-14423-9

Skamarock, W. C. et al. (2005), A description of the advanced research WRF version 2. In: NCAR Technical Note NCAR/TN-468+STR. doi:10.5065/D6DZ069T

Tanaka, K. (2010), Atmospheric pressure-wave bands around a cold front resulted in a meteotsunami in the East China Sea in February 2009. *Nat. Hazards Earth Syst. Sci., 10*, 2599–2610. doi:10.5194/nhess-10-2599-2010

Titov, V., Rabinovich, A. B., Mofjeld, H. O., Thomson, R. E., & González, F. I. (2005), The Global Reach of the 26 December 2004 Sumatra Tsunami, *Science*, *309*(5743), 2045-2048. doi:10.1126/science.1114576

Titov, V. & Moore, C. (2021), Meteotsunami model forecast: can coastal hazard be quantified in real time?. *Nat. Hazards*. doi:10.1007/s11069-020-04450-6

Tojčić, I., Denamiel, C., & Vilibić, I. (2021), Performance of the Adriatic early warning system during the multi-meteotsunami event of 11–19 May 2020: an assessment using energy banners, *Nat. Hazards Earth Syst. Sci. Discuss.*, preprint in review. doi:10.5194/nhess-2020-409

Vilibić, I., Šepić, J., Dunić, N., Sevault, F., Monserrat, S., & Jordà, G. (2018), Proxy-based assessment of strength and frequency of meteotsunamis in future climate. *Geophys. Res. Lett.*, *45*, 10501–10508. doi:10.1029/2018GL079566

Vilibić, I., & Šepić, J. (2017), Global mapping of nonseismic sea level oscillations at tsunami timescales. *Sci. Rep.*, ***7***, 40818. doi:10.1038/srep40818

Vilibić, I., Šepić, J., Rabinovich, A. B., & Monserrat, S. (2016), Modern approaches in meteotsunami research and early warning. *Front. Mar. Sci.*, *3*, 57. doi:10. 3389/fmars.2016.00057

Vilibić, I., & Šepić, J. (2009), Destructive meteotsunamis along the eastern Adriatic coast: Overview. *Phys. Chem. Earth*, *34*, 904–917.

Vučetić, T., Vilibić, I., Tinti, S., & Maramai, A. (2009), The Great Adriatic flood of 21 June 1978 revisited: An overview of the reports. *Phys. Chem. Earth*, *34*, 894–903.

Warner, J. C., Armstrong, B., He, R., & Zambon, J. B. (2010), Development of a Coupled Ocean-Atmosphere-Wave-Sediment Transport (COAWST) modeling system. *Ocean Modell.*, *35*, 230–244. doi:10.1016/j.ocemod.2010.07.010

Wertman, C. A., Yablonsky, R. M., Shen, Y., Merrill, J., Kincaid, C. R., & Pockalny, R. A. (2014), Mesoscale convective system surface pressure anomalies responsible for meteotsunamis along the U.S. East Coast on June 13th, 2013. *Sci. Rep.*, *4*, 7143. doi:10.1038/srep07143

Williams, D. A., Horsburgh, K. J., Schultz, D. M., & Hughes, C. W. (2020), Proudman resonance with tides, bathymetry and variable atmospheric forcings, *Nat Hazards*. doi:10.1007/s11069-020-03896-y